DEBIASED AND DENOISED PROJECTION LEARNING FOR INCOMPLETE MULTI-VIEW CLUSTERING

Anonymous authors
Paper under double-blind review

ABSTRACT

Multi-view clustering achieves outstanding performance but relies on the assumption of complete multi-view samples. However, certain views may be partially unavailable due to failures during acquisition or storage, resulting in distribution shifts across views. Although some incomplete multi-view clustering (IMVC) methods have been proposed, they still confront the following limitations: 1) Missing-view data imputation methods increase the unnecessary computational complexity; 2) Consensus representation imputation methods always ignore the inter-view distribution bias due to missing views. To tackle these issues, we propose a novel IMVC based on Debiased and Denoised Projection (DDP-IMVC) learning. Specifically, it utilizes the unbiased projection learned from complete views to refine the biased projection learned from data with missing views. Additionally, we introduce a robust contrastive learning for consensus projection to mitigate cluster collapse risk induced by misalignment noise. Comprehensive experiments demonstrate that DDP-IMVC achieves superior performance compared with state-of-the-art methods.

1 INTRODUCTION

Multi-view clustering (MVC) has achieved significant breakthroughs in the field of unsupervised learning (Fang et al., 2023; Yan et al., 2024b; Zhang et al., 2024a). Unfortunately, the superior performance of existing MVC methods largely relies on the assumption of complete cross-view samples. However, due to failures during data acquisition or storage, partial data in some views may be unavailable, leading to distributional shifts across views. As a result, existing MVC methods are inapplicable for incomplete multi-view data. Therefore, the problem of incomplete multi-view clustering (IMVC) has attracted increasing attention (Xu et al., 2024; Dong et al., 2024; Wan et al., 2024). The goal of IMVC is to uncover the common clustering patterns hidden in incomplete multi-view data and to group unlabeled instances into distinct clusters.

Existing IMVC methods can be categorized into two types: traditional methods and deep methods. Many traditional IMVC methods have achieved notable advances. They typically impute the missing data and then adopt machine learning techniques to explore cluster information. These methods can be further divided into three subcategories: kernel-based methods (Liu et al., 2019; 2020), matrix factorization-based methods (Hu & Chen, 2019; Chao et al., 2022), and graph learning-based methods (Wen et al., 2019; Li et al., 2022). However, the performance of traditional IMVC methods largely depends on the quality of features. Although they are more interpretable than deep methods, their representational capacity is often weaker.

Owing to the powerful generalization and representation capabilities of deep neural networks, deep IMVC methods have achieved outstanding performance. Some prototype-matching-based methods (Liu et al., 2022; Jin et al., 2023) learn a certain number of prototypes from the available data and then establish correspondences to recover missing data. However, due to cross-view data heterogeneity, networks may produce inconsistent cluster centers, leading to mismatches between samples and prototypes. Other methods attempt to complete missing views by leveraging the latent features of cross-view neighbors (Chao et al., 2024; 2025). Nevertheless, these approaches overlook the global information of samples, which introduces substantial cross-view misalignment noise when the missing rate is high. Some studies even simply fill in the missing data using the learned consensus representations (Lin et al., 2022; Yin et al., 2025). Such incorrect correspondences may further exacerbate distribution shifts and result in erroneous clustering structures.

It can be observed that deep IMVC still encounters two major challenges: 1) Existing methods often ignore the complementary role of the available views in incomplete samples when learning their consensus representation. Unfortunately, although a few approaches have considered this issue, they usually lack effective strategies to mitigate the distribution shifts induced by missing views. 2) Existing methods tend to simply restore or complete data using the learned consensus representation. While the consensus representation captures certain cross-view consistencies, the absence of necessary structural consistency constraints inevitably introduces misalignment noise. This, in turn, exacerbates the risk of clustering collapse.

To address the above issues, we propose a novel strategy based on debiased and denoised projection learning for incomplete multi-view clustering. The proposed framework is illustrated in Figure 1. Notably, our consensus learning paradigm is not merely restricted to intra-view or inter-view interactions, but instead enables concurrent interactions across all instances. Specifically, to bridge the semantic gaps across views, DDP-IMVC optimizes the projections of the common embedding space by maximizing the mutual information between the consensus projections and the view-specific embeddings. In practice, we design adaptive projection matrices based on cluster separability to collaboratively integrate detailed information from all views and to accommodate the influence of varying degrees of missing instances. In this space, an unbiased projection is introduced through a refinement strategy to correct biased projections, thereby constructing robust consensus projections. Furthermore, to overcome the heterogeneity in IMVC and inconsistencies of consensus projections, DDP-IMVC employs a denoised contrastive strategy to reduce the risk of clustering collapse. Finally, the data are recovered through the matched consensus projections. Our main contributions can be summarized as follows:

- We propose an innovative incomplete multi-view clustering framework, i.e., DDP-IMVC, which employs unbiased projection to correct and refine the distribution shifts of the biased projection.
- To alleviate the cluster collapse problem induced by misalignment noise, we adopt a robust contrastive constraint based on consensus projections. This approach facilitates the generation of common embedding projections.
- We analyze the robustness of DDP-IMVC from both theoretical and experimental perspectives. Extensive experiments demonstrate that under varying missing rates, DDP-IMVC significantly outperforms state-of-the-art methods across four datasets.

2 Related Work

2.1 Multi-View clustering

MVC groups samples with similar feature patterns into the same cluster by integrating feature information from different views (Yang & Wang, 2018; Zhou et al., 2024). Deep autoencoders, as powerful feature extraction tools, have been widely applied in MVC. To address the inconsistency between discrete clustering information and continuous visual information, Xu et al. (2021) employs a variational autoencoder to learn disentangled representations. MFLVC relies on an autoencoder to learn latent features at different levels to mine common semantics (Xu et al., 2022b). However, these methods struggle to eliminate the interference of private information and noise during consistent information extraction. Yan et al. (2024a) proposes a novel variational autoencoder under information bottleneck theory to preserve clustering information. Unlike the above approaches that optimize reconstruction loss to learn latent features, Xie et al. (2020) constructs a multi-view joint clustering network using stacked autoencoders, convolutional autoencoders, and variational autoencoders to capture precise multi-view features. Trosten et al. (2021); Tang & Liu (2022) employ encoding networks to extract view-specific features while maintaining cluster compactness through clustering constraints. Moreover, for real-world multi-view data with missing views, the above methods often struggle to uncover accurate data representations. Therefore, uncovering accurate clustering patterns in incomplete multi-view data has become an important research direction.

2.2 Incomplete Multi-View Clustering

In recent years, IMVC has achieved significant breakthroughs. Generally, deep IMVC methods can be divided into four categories: 1)Prediction-based methods. Lin et al. (2021; 2022) predict the missing data with the predictor to leverage the available data across views, with the goal of minimizing the conditional entropy. 2) Adversarial network-based methods. Wang et al. (2021) explicitly generates missing view data through generative adversarial networks (GANs) and integrates multi-view information to achieve efficient clustering. Wang et al. (2023) proposes a self-supervised framework that combines GANs with dual contrastive learning, exploiting the hidden information in incomplete data. 3)Prototype-based methods. Dai et al. (2025) proposes an IMVC framework in a common semantic space based on consensus semantics without data completion or alignment. Yuan et al. (2025) introduces a robust prototype contrastive strategy to handle overfitting caused by prototype misalignment. 4)Neighborhood-based methods. Tang & Liu (2022) dynamically updates neighbors based on learned semantic features, avoiding the interference of low-quality samples during data completion. Chao et al. (2024) constructs a neighbor-sample adjacency matrix and adopts graph neural networks (GNNS) to complete missing samples. Pu et al. (2024) constructs a latent graph to preserve topological information for the dynamic imputation of missing embedded features. Chao et al. (2025) adaptively completes missing representations by integrating intra-view local relationships and cross-view global relationships through GCNs. Despite their effectiveness, most IMVC methods ignore the potential inter-view distribution bias due to missing views.

3 Methodology

3.1 Notations

Given a multi-view dataset $\mathcal{X} = \{\mathbf{X}^v \in \mathbb{R}^{N\times D_v}\}_{v=1}^V$, consisting of N samples, each represented by V views of dimensionality D_v. There are N_u complete samples with all views and N_b samples with missing values. Let the complete samples be denoted as $\{\mathbf{X}_\mathrm{C}^v\}_{v=1}^V$, and the samples with missing views be denoted as $\{\mathbf{X}_\mathrm{I}^v\}_{v=1}^V$. A complete view indicator matrix $\mathbf{M} \in \{0,1\}^{N\times V}$ indicates the positions of missing views. $\mathbf{M}_{iv}$ is set to 1 if the i-th sample in the v-th view is observed; otherwise, it indicates a missing view. It is assumed that no sample is missing in all views simultaneously, i.e., $\forall i \in \{1,\dots,N\}, \sum_{v=1}^V \mathbf{M}_{iv} \geq 1$. The task is to cluster these N samples with potentially missing views into K clusters.

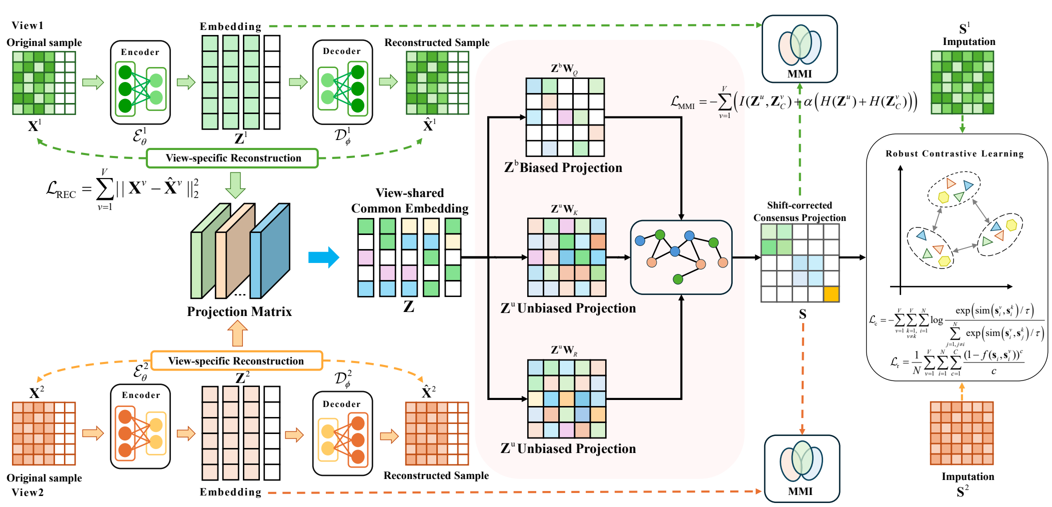

Figure 1: The architecture of our proposed DDP-IMVC framework. (a) Independent autoencoders are employed for each view to extract deep features. (b) The deep features are adaptively projected in a consensus embedding space to bridge the semantic gaps across views. (c) An attention-based refinement strategy is employed to optimize the biased projection introduced by the incomplete sample. (d) A denoised consensus projection contrastive strategy is adopted to alleviate the risk of clustering collapse.

3.2 VIEW-SPECIFIC RECONSTRUCTION

Considering that the data across different views are mostly heterogeneous and differently distributed, we provide independent autoencoders for each view to alleviate clustering instability on the manifold structure in high-dimensional space (Hinton & Salakhutdinov, 2006; Guo et al., 2017). An autoencoder $\mathcal{E}_\theta^v(\cdot)$ is used to learn the embedding of the sample:

$$\mathbf{Z}^v = \mathcal{E}_\theta^v(\mathbf{X}^v), \tag{1}$$

where $\mathbf{Z}^v \in \mathbb{R}^{N\times d}$ denotes the embedding of the v-th view in the d-dimensional embedding space. θ represents the learnable parameters of the autoencoder. Then, we reconstruct the embedding $\mathbf{Z}^v$ into $\hat{\mathbf{X}}^v \in \mathbb{R}^{N\times D_v}$ with the decoder $\mathcal{D}_\phi^v(\cdot)$, as follows:

$$\hat{\mathbf{X}}^v = \mathcal{D}_\phi^v(\mathbf{Z}^v), \tag{2}$$

where ϕ denotes the learnable parameters of the decoder. The reconstruction loss across all views can be expressed as follows:

$$\mathcal{L}_{\text{REC}} = \sum_{v=1}^{V} ||\mathbf{X}^v - \hat{\mathbf{X}}^v||_2^2. \tag{3}$$

3.3 UNBAISED REFINEMENT FOR DEBIASED PROJECTION

Multi-view complementary information can enhance cluster separability, making single-view inseparable clusters linearly separable (Zhang et al., 2024b; Dai et al., 2025). Moreover, in the common embedding space, the view-specific projections share consistent semantics, allowing each sample to be represented by the projection from any view. Accordingly, we extract common representations through an adaptive projection matrix.

Variance reflects sample deviation from the mean along a certain dimension, with well-separated clusters exhibiting high value (Xu et al., 2023). We leverage the variance to assess the separability of clusters and compute an adaptive projection matrix $\mathbf{W} \in \mathbb{R}^{N\times V}$ that preserves the clustering information of views with well-defined cluster structures:

$$\mathbf{W}_{iv} = \frac{\text{Var}(\mathbf{Z}_\text{C}^v)}{\sum_{v'=1}^{V} \mathbf{M}_{iv'}\text{Var}(\mathbf{Z}_\text{C}^{v'})}, \tag{4}$$

where $\mathbf{W}_{iv}$ denotes the projection weight of the i-th sample in the v-th view. Var$(\cdot)$ represents the variance operator. The mask $\mathbf{M}_{iv'}$ allows the projection matrix to adapt to randomly missing data. $\mathbf{Z}^v = [\mathbf{Z}_\text{I}^v; \mathbf{Z}_\text{C}^v]$ denotes embedding representations of the complete samples and incomplete samples in the v-th view. Based on the projection matrix $\mathbf{W}$, the samples are mapped to the view-shared common embeddings $\mathbf{Z} \in \mathbb{R}^{N\times d}$.

$$\mathbf{z}_i = \sum_{v=1}^{V} \mathbf{W}_{iv}\mathbf{z}_i^v. \tag{5}$$

where $\mathbf{z}_i \in \mathbf{Z}$ denotes the projection of the i-th sample from all views.

The random missing of sample views can cause distribution shifts and lower clustering separability. To address this, we innovatively propose an attention-based complementarity refinement (Vaswani et al., 2017). The core idea is to compute the similarity between the biased projections $\mathbf{z}_i^b$ and unbiased projections $\mathbf{z}_i^u$ as sample affinity attention weights $\mathbf{A}$. It extracts the unbiased projection most compatible with the missing samples to correct the distribution shifts.

Biased projections are defined as those corresponding to samples with missing views, while unbiased projections correspond to samples with all views complete:

$$\mathbf{Z}^u = \mathbf{Z}\big[\{\, i \mid \prod_{v=1}^{V} \mathbf{M}_{iv} = 1\,\}, :\big], \tag{6}$$

$$\mathbf{Z}^b = \mathbf{Z}\big[\{\, i \mid \prod_{v=1}^{V} \mathbf{M}_{iv} = 0\,\}, :\big]. \tag{7}$$

Then, by comparing the biased projections with the high-quality unbiased projections, the corresponding affinity attention weights are computed:

$$\mathbf{A}^{(l)} = \mathrm{Softmax}\left(\frac{\mathbf{Z}^b\mathbf{W}_Q^{(l)}\left(\mathbf{Z}^u\mathbf{W}_K^{(l)}\right)^\top}{\sqrt{d/L}}\right), l = 1, 2, ..., L \tag{8}$$

where $\mathbf{W}_Q$ and $\mathbf{W}_K$ denote learnable parameters. L denotes the number of attention heads. d denotes the dimension of the projection $\mathbf{Z}$. Based on the affinity attention weights, the unbiased projections can be used to correct the data shifts present in the biased projections. Finally, the results from all attention heads are concatenated to obtain the the corrective features in the common embedding space:

$$\mathbf{B}^{(l)} = \mathbf{A}^{(l)}(\mathbf{Z}^u\mathbf{W}_R^{(l)}), \tag{9}$$

$$\mathbf{B} = [\mathbf{B}^{(1)}, ..., \mathbf{B}^{(L)}], \tag{10}$$

where $\mathbf{W}_R$ denotes learnable parameters. Then we incorporate the information of corrective features $\mathbf{B}$ into the biased projections to obtain shift-corrected consensus projections $\mathbf{S} \in \mathbb{R}^{N\times d}$:

$$\mathbf{S} = [\mathbf{Z}^u; \mathbf{Z}^b] + [\mathbf{0}; \mathbf{B}], \tag{11}$$

where $\mathbf{0}$ denotes an all-zero matrix with the same dimensions as $\mathbf{Z}^u$. Clearly, correcting the distribution shifts caused by missing data lies in the high-quality common projected embeddings. Accurate projections of multi-view features require exploiting the correlation between the view-specific features and the projected embeddings. A natural idea is to maximize the mutual information (Lin et al., 2021) between unbiased projections and embeddings under each view. Specifically, we regard the unbiased projections as the anchor of the embeddings under each view, and sequentially maximize the mutual information between the anchor and a specific view with the following loss function:

$$\mathcal{L}_{\text{MMI}} = -\sum_{v=1}^{V}\left(I(\mathbf{Z}^u, \mathbf{Z}_C^v) + \alpha\left(H(\mathbf{Z}^u) + H(\mathbf{Z}_C^v)\right)\right), \tag{12}$$

where α serves as the entropy regularization coefficient. $I(\cdot)$ denotes mutual information, and $H(\cdot)$ denotes information entropy, which can be computed as follows:

$$H(\mathbf{X}) = -\sum_x p(x)\log p(x), \tag{13}$$

$$I(\mathbf{X};\mathbf{Y}) = \sum_x\sum_y p(x,y)\log\frac{p(x,y)}{p(x)p(y)}. \tag{14}$$

where $p(x)$ denotes the probability distribution of the random variable $\mathbf{X}$, and $p(x, y)$ denotes the joint distribution of the random variables $\mathbf{X}$ and $\mathbf{Y}$.

Since the consensus projections capture both the inherent information of the incomplete samples and the clustering information of the affiliated complete sample set, restoring embedding with consensus projections can effectively ensure the integrity of the sample structure and the consistency of the distribution. Therefore, we complete the missing-view embeddings from consensus projections by:

$$\mathbf{S}^v = \mathbf{Z}^v + (1 - \tilde{\mathbf{M}}^v) \odot \mathbf{S}, \tag{15}$$

where $\odot$ denotes the element-wise multiplication. $\mathbf{S}^v$ denotes the embeddings after completion in the v-th view. We take the v-th column of matrix $\mathbf{M} \in \mathbb{R}^{N\times V}$ as $\mathbf{m}^v \in \mathbb{R}^{N\times 1}$ that indicates the missing samples in the v-th view and expand it into $\tilde{\mathbf{M}}^v \in \mathbb{R}^{N\times d}$ by replicating $\mathbf{m}^v$ d times. Finally, we project the completed embeddings $\mathbf{S}^v$ into $\mathbf{S}'$ via the variance projection matrix, which is constructed by leveraging the variance of the embeddings from each view.

3.4 Dual Contrastive Learning for Denoised Projection

3.4.1 Inter-view Contrastive Learning

To overcome the heterogeneity in incomplete multi-view learning, we construct positive pairs from the same instance across views and negative pairs from different instances. Contrastive learning maximizes the positive-pair correlation while minimizing that of negative pairs. The contrastive learning loss across all views is:

$$\mathcal{L}_{\text{c}} = -\sum_{v=1}^{V}\sum_{\substack{k=1,\\ v\neq k}}^{V}\sum_{i=1}^{N}\log\frac{\exp\left(\text{sim}\left(\mathbf{s}_i^v,\mathbf{s}_i^k\right)/\tau\right)}{\sum_{j=1,j\neq i}^{N}\exp\left(\text{sim}\left(\mathbf{s}_i^v,\mathbf{s}_j^k\right)/\tau\right)}, \tag{16}$$

where $\mathbf{s}_i^v$ and $\mathbf{s}_j^k$ denote the representations from v-th view and k-th view. $\text{sim}(\cdot)$ is cosine similarity. τ represents the temperature coefficient.

3.4.2 Robust Contrastive Learning

To prevent cluster collapse after completing missing views with consensus projections, it is necessary to impose constraints between the consensus projections and the recovered samples. A conventional approach is to apply contrastive learning between them. Although consensus projections capture the consistency of the data distribution, the completion process inevitably introduces potential noise. Conventional contrastive learning's strong focus on hard samples can exacerbate noise-induced overfitting. Inspired by Yuan et al. (2024), we employ a denoised contrastive learning between consensus projection $\mathbf{S}$ and each view projection $\mathbf{S}^v$ to enhance the robustness of consensus projections against noise.

Set $f(\mathbf{s}_i,\mathbf{s}_j) = \frac{\exp(\text{sim}(\mathbf{s}_i,\mathbf{s}_j)/\tau)}{\sum_{n=1}^{N}\exp(\text{sim}(\mathbf{s}_i,\mathbf{s}_n)/\tau)}$, and thus $\sum_{j=1}^{N} f(\mathbf{s}_i,\mathbf{s}_j) = 1$. For the general form of InfoNCE, its power series expansion over the interval $[0,1]$ is:

$$\begin{aligned}
\mathcal{L}_{\text{Info}} &= -\frac{1}{N}\sum_{v=1}^{V}\sum_{i=1}^{N}\log\frac{\exp\left(\text{sim}(\mathbf{s}_i,\mathbf{s}_i^v)/\tau\right)}{\sum_{n=1}^{N}\exp\left(\text{sim}(\mathbf{s}_i,\mathbf{s}_n^v)/\tau\right)}\\
&= \frac{1}{N}\sum_{v=1}^{V}\sum_{i=1}^{N}\left[(1-f(\mathbf{s}_i,\mathbf{s}_i^v)) + \frac{(1-f(\mathbf{s}_i,\mathbf{s}_i^v))^2}{2} + \ldots + \frac{(1-f(\mathbf{s}_i,\mathbf{s}_i^v))^c}{c} + \ldots\right]\\
&= \frac{1}{N}\sum_{v=1}^{V}\sum_{i=1}^{N}\left[\frac{1}{2}(2-2f(\mathbf{s}_i,\mathbf{s}_i^v)) + \frac{(1-f(\mathbf{s}_i,\mathbf{s}_i^v))^2}{2} + \ldots + \frac{(1-f(\mathbf{s}_i,\mathbf{s}_i^v))^c}{c} + \ldots\right]\\
&= \frac{1}{N}\sum_{v=1}^{V}\sum_{i=1}^{N}\left[\frac{1}{2}||\mathbf{e}_i-\mathbf{f}_i||_1 + \frac{(1-f(\mathbf{s}_i,\mathbf{s}_i^v))^2}{2} + \ldots + \frac{(1-f(\mathbf{s}_i,\mathbf{s}_i^v))^c}{c} + \ldots\right]\\
&= \frac{1}{2N}\sum_{v=1}^{V}\sum_{i=1}^{N}||\mathbf{e}_i-\mathbf{f}_i||_1 + \frac{1}{N}\sum_{v=1}^{V}\sum_{i=1}^{N}\sum_{c=1}^{\infty}\frac{(1-f(\mathbf{s}_i,\mathbf{s}_i^v))^c}{c}
\end{aligned} \tag{17}$$

where $\mathbf{e}_i$ denotes the one-hot encoding whose i-th element is 1; $\mathbf{f}_i$ is a vector whose the j-th element is $f(\mathbf{s}_i,\mathbf{s}_i^v)$. It can be seen that, after expanding InfoNCE into an infinite series, the first term is exactly the Mean Absolute Error (MAE) loss, which is proven to be robust to noise (Ghosh et al., 2015; 2017). However, MAE loss treats each sample equally. The infinite terms can provide differentiated attention to samples but are sensitive to noise. Therefore, we can construct a robust contrastive loss by truncating part of the infinite series to maintain a balance between MAE loss and InfoNCE loss, which is adjusted by a truncation coefficient C. Specifically, we take the first C terms of the infinite series and obtain the robust contrastive loss as follows:

$$\mathcal{L}_{\text{r}} = \frac{1}{N}\sum_{v=1}^{V}\sum_{i=1}^{N}\sum_{c=1}^{C}\frac{(1-f(\mathbf{s}_i,\mathbf{s}_i^v))^c}{c}, \tag{18}$$

Its significance lies in that it transforms the unbounded amplification of $-\log f(\mathbf{s}_i,\mathbf{s}_i^v)$ for hard samples into a bounded approximation, balancing positive sample discrimination and noise suppression. Adjusting the truncation coefficient C allows tuning between cluster collapse and noise robustness.

Finally, the dual contrastive loss is:

$$\mathcal{L}_{\text{DCL}} = \mathcal{L}_{\text{c}} + \mathcal{L}_{\text{r}}. \tag{19}$$

Algorithm 1 DDP for Incomplete Multi-view Clustering

1: **Input**: Incomplete multi-view dataset $\mathcal{X} = \{\mathbf{X}^v\}_{v=1}^V$ for all N samples, Training epoch E, Hyper-parameter λ_1, λ_2, α, and C.
2: Construct the complete view indicator matrix $\mathbf{M} \in \mathbb{R}^{N \times V}$.
3: **while** Not reaching epochs E **do**
4: Calculate the embedding representation $\{\mathbf{Z}^v\}_{v=1}^V$ by Eq.(1).
5: Calculate the projection embedding $\mathbf{Z}$ by Eq.(5).
6: Correct the shifts to obtain consensus projections $\mathbf{S}$ by Eq.(11).
7: Impute the each view embeddings $\mathbf{S}^v$ by Eq.(15).
8: Compute the clustering-friendly representation $\mathbf{S}'$ with the imputed embeddings.
9: Optimize the total loss function $\mathcal{L}_{all}$ by Eq.(20).
10: **end while**
11: Perform k-means clustering algorithm on $\mathbf{S}'$.
12: **Output**: K clusters for N samples.

3.5 The Objective Function

Overall, the total loss function of our method consists of three parts are formulated as:

$$\mathcal{L}_{all} = \mathcal{L}_{\text{REC}} + \lambda_1 \mathcal{L}_{\text{MMI}} + \lambda_2 \mathcal{L}_{\text{DCL}}. \tag{20}$$

λ_1 and λ_2 are trade-off parameters. $\mathcal{L}_{\text{REC}}$ is the autoencoder reconstruction loss. $\mathcal{L}_{\text{MMI}}$ is the maximum mutual information loss, used to enhance the common cluster information. $\mathcal{L}_{\text{DCL}}$ is the robust contrastive loss that mitigates heterogeneity in incomplete multi-view learning and prevents cluster collapse. Finally, K-means is performed on $\mathbf{S}^{'} \in \mathbb{R}^{N \times d}$ to obtain K clusters.

4 Experiments

4.1 Datasets

We conducted experiments on four representative datasets. The datasets are: **HandWritten** (LeCun et al., 1989) comprises 2,100 samples belonging to 10 categories corresponding to digits from 0 to 9. We employ three distinct features Pixel, Fourier and Profile for analysis. **Scene-15** (Fei-Fei & Perona, 2005) consists of 15 categories with a total of 4,485 samples. GIST, PHOG, and LBP are selected as three views in our experiments. **ALOI-100** (Geusebroek et al., 2005) contains 10,800 object images belonged to 100 categories. We extract HSB, RGB, Colorsim, and Haralick features to construct multi-view data. **LandUse-21** (Yang & Newsam, 2010) comprises 2,100 samples belonging to 21 categories corresponding to different land-use scene categories. GIST, PHOG and LBP are used for analysis. To evaluate the performance of our approach, we employ three standard metrics: Accuracy (ACC), Normalized Mutual Information (NMI), and Adjusted Rand Index (ARI).

4.2 Compare Method

DDP-IMVC is compared with nine SOTA methods. **Fusion-kmeans** clusters the mean-fused features with k-means. **Completer** (Lin et al., 2021) predicts missing views by minimizing conditional entropy. **DIMVC** (Xu et al., 2022a) proposes a no-imputation framework that maps data to reveal linear separability. DSIMVC (Tang & Liu, 2022) completes views by dynamically mining semantic features of neighbors. **DCP** (Lin et al., 2022) learns consistent representations via dual contrastive learning under the information-theoretic framework. **ProImp** (Li et al., 2023) recover data by learning prototypes with dual attention layers. **APADC** (Xu et al., 2023) achieves imputation-free stragedy through adaptive projection and distribution alignment. **ICMVC** (Chao et al., 2024) completes missing views with GNNs and aligns distributions through high confidence guidance. **GHICMC** (Chao et al., 2025) employs cascaded GNNs to enable global graph propagation and hierarchical information transfer.

Table 1: Clustering results of all methods on four datasets. The best and second-best results are highlighted with bold and underline, respectively.

	Missing_rates	0.1			0.3			0.5			0.7		
	Metrics	ACC	NMI	ARI	ACC	NMI	ARI	ACC	NMI	ARI	ACC	NMI	ARI
LandUse-21	Fusion-kmeans	20.45	25.42	8.62	16.41	17.48	5.51	12.86	12.58	2.77	11.45	9.81	1.38
	Completer(2021)	26.40	32.48	13.93	26.96	32.64	12.09	21.36	26.27	9.34	24.43	**29.01**	10.31
	DIMVC(2022)	24.63	30.04	10.58	23.69	29.94	10.01	22.40	27.78	9.38	21.77	26.14	7.91
	DSIMVC(2022)	18.47	19.34	5.58	17.95	18.47	5.16	18.13	18.53	5.26	17.90	17.97	5.11
	DCP(2023)	26.78	30.87	13.80	27.08	30.69	13.80	23.07	27.00	11.31	25.18	28.04	**12.00**
	ProImp(2023)	22.38	23.79	8.76	19.53	20.55	6.86	20.30	21.94	7.32	15.10	15.48	4.00
	APADC(2023)	22.75	31.90	9.50	18.08	24.72	7.22	15.67	21.23	5.61	15.11	20.08	4.84
	ICMVC(2024)	28.18	31.78	**15.14**	25.77	29.39	12.69	25.98	27.74	11.92	22.26	24.95	9.31
	GHICMC(2025)	26.86	31.14	12.81	25.72	29.26	11.32	25.15	28.57	11.26	23.53	26.55	9.72
	Ours	**28.21**	**34.68**	14.93	**28.02**	**33.49**	**14.27**	**27.14**	**31.89**	**13.24**	**25.36**	28.09	10.67
Scene-15	Fusion-kmeans	34.20	34.84	20.93	22.39	23.60	12.80	17.54	17.31	7.88	14.90	13.54	4.29
	Completer(2021)	40.28	42.50	23.13	40.12	42.93	23.96	39.12	41.79	22.98	38.05	40.22	21.84
	DIMVC(2022)	32.95	27.41	15.61	33.51	29.42	16.75	30.65	25.21	13.64	29.58	24.11	12.85
	DSIMVC(2022)	27.65	29.74	14.11	26.73	29.36	13.94	26.40	28.03	13.04	25.31	27.04	12.43
	DCP(2023)	38.54	42.39	23.33	40.49	43.10	24.14	39.50	42.35	23.51	38.55	40.57	21.72
	ProImp(2023)	40.74	42.14	24.00	41.69	43.03	25.28	40.28	41.80	23.89	39.96	40.35	22.92
	APADC(2023)	43.70	44.20	26.00	41.80	43.10	24.30	39.90	42.40	23.80	38.50	41.10	22.80
	ICMVC(2024)	38.78	36.62	21.84	37.40	34.94	20.60	31.35	27.91	14.98	25.31	23.88	11.33
	GHICMC(2025)	41.26	43.21	24.95	40.98	43.13	25.05	40.91	42.29	24.64	38.79	40.94	22.92
	Ours	**46.16**	**47.62**	**28.69**	**45.53**	**45.99**	**28.05**	**44.35**	**43.67**	**26.79**	**42.12**	**41.20**	**24.73**
HandWritten	Fusion-kmeans	41.70	47.59	34.22	36.28	38.76	21.46	29.64	28.51	11.54	25.69	22.14	6.58
	Completer(2021)	83.22	82.47	73.59	75.38	77.55	61.69	74.05	76.13	58.89	78.55	76.07	68.67
	DIMVC(2022)	67.13	63.17	53.16	59.43	56.49	43.19	54.80	50.50	30.76	43.82	41.54	23.80
	DSIMVC(2022)	84.35	80.32	74.38	85.64	80.71	75.94	84.73	78.82	74.13	82.71	75.35	69.85
	DCP(2023)	53.35	65.72	35.60	51.96	63.88	31.49	59.06	65.07	36.51	60.97	60.53	29.90
	ProImp(2023)	83.20	80.29	74.17	84.24	77.75	72.60	78.16	70.79	63.96	80.31	68.85	62.92
	APADC(2023)	67.43	65.34	47.18	68.95	67.28	45.98	68.85	68.61	56.43	61.77	61.97	48.26
	ICMVC(2024)	83.16	81.33	74.78	82.01	79.62	72.22	75.13	71.99	63.19	72.47	70.01	59.71
	GHICMC(2025)	96.19	92.14	**92.89**	96.11	91.32	90.83	**94.88**	**89.16**	**89.10**	**92.73**	**85.85**	**84.71**
	Ours	**96.38**	**92.23**	91.99	**96.15**	**91.49**	**91.21**	94.34	88.38	87.87	90.86	82.65	81.92
ALOI-100	Fusion-kmeans	52.37	72.31	40.79	30.63	55.28	16.10	22.48	47.33	7.46	17.39	41.82	4.94
	Completer(2021)	48.19	77.96	44.25	43.03	72.43	36.73	36.16	66.89	26.52	34.55	64.06	24.97
	DIMVC(2022)	71.86	84.99	61.79	68.52	82.15	58.31	64.80	78.53	51.36	61.64	75.33	47.25
	DSIMVC(2022)	38.76	67.49	29.71	38.89	66.00	29.12	39.32	64.42	28.53	35.98	61.28	25.16
	DCP(2023)	51.85	74.88	42.73	47.38	70.54	38.38	42.37	66.30	32.36	36.02	60.75	25.40
	ProImp(2023)	68.39	83.47	62.08	45.98	73.01	38.53	32.71	65.74	24.76	29.23	62.08	19.46
	APADC(2023)	47.40	68.92	35.02	38.95	62.27	26.10	32.78	58.16	20.10	26.02	53.91	14.11
	ICMVC(2024)	68.02	80.78	56.64	68.14	80.40	55.94	67.68	78.92	53.92	49.15	70.50	38.45
	GHICMC(2025)		OOM			OOM			OOM			OOM	
	Ours	**76.02**	**88.35**	**67.82**	**73.18**	**85.82**	**64.36**	**69.87**	**82.34**	**58.09**	**66.94**	**78.60**	**53.20**

Table 2: Ablation study results on LandUse21 and Scene-15 datasets with missing rate 0.3.

Datasets			LandUse21			Scene-15		
$\mathcal{L}_{\text{REC}}$	$\mathcal{L}_{MMI}$	$\mathcal{F}_{DCL}$	ACC	NMI	ARI	ACC	NMI	ARI
✓		✓	17.54	22.97	6.08	36.06	43.69	21.88
✓	✓		24.16	26.09	11.06	41.96	40.00	25.94
✓			16.78	17.96	5.63	21.53	21.61	11.48
✓	✓	✓	**28.02**	**33.49**	**14.27**	**45.53**	**45.99**	**28.05**

4.3 Experimental Settings

We adopt Adam to optimize our framework DDP-IMVC and all the experiments are conducted in PyTorch 1.13.1 on Windows with an NVIDIA 4070 SUPER GPU. The dimensions of encoders are D_v–1024–1024–1024–128. The decoder is symmetric to its corresponding encoder. The number of heads L in multi-head attention is set to 4. The entropy regularization coefficient α is set to 10, and the truncation coefficient C is set to 9.

4.4 Incomplete Multi-View Clustering Performance

Table 1 reports the incomplete multi-view clustering results of all methods under different missing rates. It shows that DDP-IMVC can effectively handle high missing rates and large-scale issues in

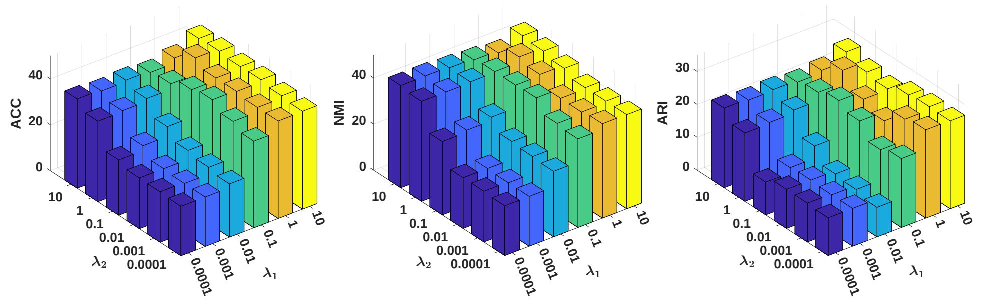

(a) ACC (b) NMI (c) ARI

Figure 2: Parameter sensitivity analysis on Scene-15 with the missing rate 0.3.

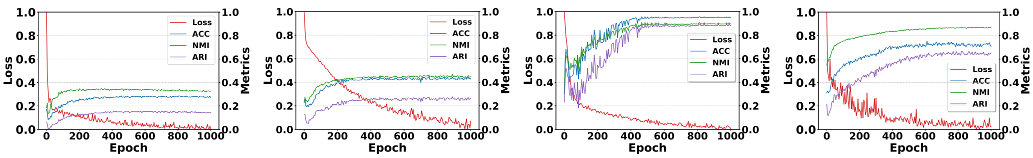

(a) LandUse-21 (b) Scene-15 (c) HandWritten (d) ALOI-100

Figure 3: The convergence analysis on all datasets with the missing rate 0.3.

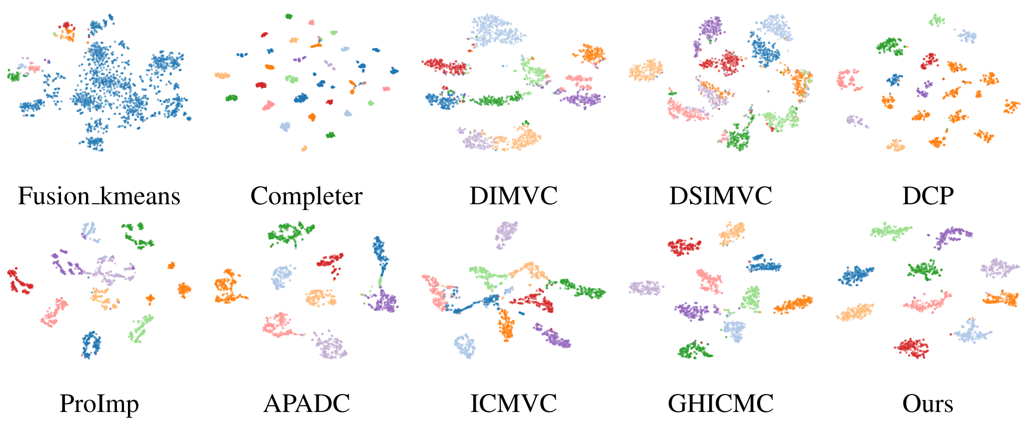

Figure 4: The visualization results of HandWritten dataset in all methods with a missing rate of 0.5.

IMVC. From the perspective of effectiveness, our method significantly outperforms SOTA methods across four datasets. For example, in Scene-15 dataset, ACC, NMI, and ARI outperform the second-best method, APADC, by an average of 3.56%, 1.92%, and 2.86%, respectively. We notice that when the missing rate is 0.5 and 0.7, DDP-IMVC performs slightly worse than GHICMC. We attribute this to the simplicity of the HandWritten dataset, where inter-class features are singular. Under high missing rates, it is suitable to use cascade graphs for data recovery. For other complex datasets, GHICMC shows a significant performance drop. More critically, its high memory consumption prevents it from handling large-scale datasets. From the perspective of robustness, DDP-IMVC can still maintain a high level of performance under a high missing rate. Moreover, unlike some methods whose performance drops sharply, DDP-IMVC remains stable even as the missing rate increases.

4.5 Model Discussion

1) Ablation Study: To investigate the importance of each component, we conducted an ablation study on our DDP-IMVC framework using LandUse21 and Scene-15 datasets under a missing rate of 0.3. As shown in Table 2, removing the attention correction mechanism for the learned consensus projection ($\mathcal{L}_{\text{MMI}}$) or the robust contrastive learning ($\mathcal{L}_{\text{DCL}}$) leads to suboptimal performance. When

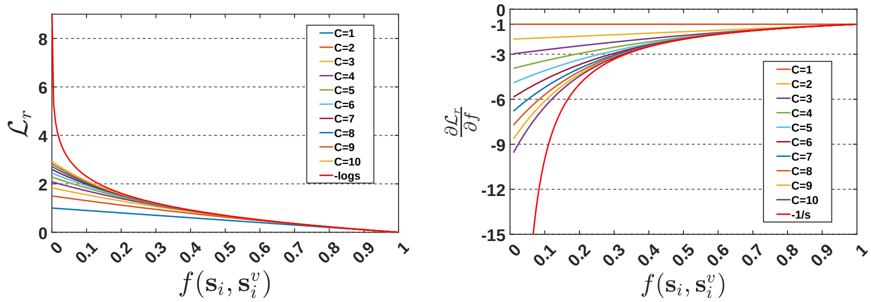

(a) (b)

Figure 5: The variation trend of the loss and its gradient.

all strategies are applied together, we achieve the best results. The experimental findings demonstrate that the attention correction mechanism can refine the distribution of biased projections, while the robust contrastive learning enhances the consistency of consensus projections and alleviates the risk of cluster collapse.

2) Parameter Analysis: Our objective loss mainly involves two trade-off parameters, λ_1 and λ_2. To verify their effectiveness, we conducted a parameter analysis by setting both parameters in the range from 10^{-4} to 10. As shown in Figure 2, excessively high or low parameter values are unfavorable for clustering. Based on our parameter experiments, we recommend setting the parameter range between 1 and 10.

3) Convergence Analysis: Meanwhile, to better verify the convergence and robustness of our model, we observed the convergence performance of all datasets under a 0.3 missing rate. As shown in the Figure 3, the total loss function involved in our training achieved excellent convergence. With the increase in training epochs, various metrics for evaluating clustering also tended to converge.

4) Visualization Analysis: As shown in Figure 4, with a missing rate of 0.5, we visualized the distribution of common embedding of all methods on the HandWritten dataset using t-SNE. Through the correction of the distribution shift of missing samples during the imputation process by DDP-IMVC, our method is facilitated to discover the common clustering patterns of all views in the common embedding space.

5) Discussion of Robust Contrastive Loss: In Figure 5, we plot the InfoNCE loss and the loss function in Equation (18), as well as their gradients. As described in Section 4.5, the single-sample InfoNCE function is $\mathcal{L}_r = -\log f$, with gradient $\frac{\partial \mathcal{L}_r}{\partial f} = -\frac{1}{f}$. The function in Equation (18) is $\mathcal{L} = \sum_{c=1}^{C} \frac{(1-f)^c}{c}$, with gradient $\frac{\partial \mathcal{L}_r}{\partial f} = -\sum_{c=1}^{C} (1-f)^{c-1}$. When $C = 1$, the gradient of Equation (18) is -1, indicating that it treats all samples equally, equivalent to MAE. When $C \to \infty$, it degenerates to InfoNCE, giving excessively high attention to noisy samples. Our loss gradient is smaller than MAE, which indicates that our loss can assign different attention levels to different samples, improving training efficiency. It is larger than InfoNCE and has an upper bound, indicating that our loss prioritizes clean samples, mitigating the issue of excessive attention to hard samples, thereby enhancing robustness.

5 Conclusion

In this work, we propose a consensus projection refinement strategy for IMVC to address data shift and misalignment noise introduced by missing views. An adaptive feature projection constructs a common embedding space. Within this space, unbiased projections correct the distribution of biased projections through an attention mechanism to form robust consensus embeddings. In addition, we employ a denoise contrastive strategy to prevent cluster collapse that may occur when completing missing views in the consensus projections. The effective synergy of these two strategies enables DDP-IMVC to achieve strong performance across most complex IMVC tasks.

References

Guoqing Chao, Songtao Wang, Shiming Yang, Chunshan Li, and Dianhui Chu. Incomplete multi-view clustering with multiple imputation and ensemble clustering. *Applied Intelligence*, 52(13): 14811–14821, 2022.

Guoqing Chao, Yi Jiang, and Dianhui Chu. Incomplete contrastive multi-view clustering with high-confidence guiding. In *Proceedings of the AAAI conference on artificial intelligence*, volume 38, pp. 11221–11229, 2024.

Guoqing Chao, Kaixin Xu, Xijiong Xie, and Yongyong Chen. Global graph propagation with hierarchical information transfer for incomplete contrastive multi-view clustering. In *Proceedings of the AAAI Conference on Artificial Intelligence*, volume 39, pp. 15713–15721, 2025.

Yuzhuo Dai, Jiaqi Jin, Zhibin Dong, Siwei Wang, Xinwang Liu, En Zhu, Xihong Yang, Xinbiao Gan, and Yu Feng. Imputation-free and alignment-free: Incomplete multi-view clustering driven by consensus semantic learning. In *Proceedings of the Computer Vision and Pattern Recognition Conference*, pp. 5071–5081, 2025.

Zhibin Dong, Jiaqi Jin, Yuyang Xiao, Bin Xiao, Siwei Wang, Xinwang Liu, and En Zhu. Subgraph propagation and contrastive calibration for incomplete multiview data clustering. *IEEE Transactions on Neural Networks and Learning Systems*, 2024.

Uno Fang, Man Li, Jianxin Li, Longxiang Gao, Tao Jia, and Yanchun Zhang. A comprehensive survey on multi-view clustering. *IEEE Transactions on Knowledge and Data Engineering*, 35 (12):12350–12368, 2023.

Li Fei-Fei and Pietro Perona. A bayesian hierarchical model for learning natural scene categories. In *2005 IEEE computer society conference on computer vision and pattern recognition (CVPR'05)*, volume 2, pp. 524–531. IEEE, 2005.

Jan-Mark Geusebroek, Gertjan J Burghouts, and Arnold WM Smeulders. The amsterdam library of object images. *International Journal of Computer Vision*, 61(1):103–112, 2005.

Aritra Ghosh, Naresh Manwani, and PS Sastry. Making risk minimization tolerant to label noise. *Neurocomputing*, 160:93–107, 2015.

Aritra Ghosh, Himanshu Kumar, and P Shanti Sastry. Robust loss functions under label noise for deep neural networks. In *Proceedings of the AAAI conference on artificial intelligence*, volume 31, 2017.

Xifeng Guo, Long Gao, Xinwang Liu, and Jianping Yin. Improved deep embedded clustering with local structure preservation. In *Ijcai*, volume 17, pp. 1753–1759, 2017.

Geoffrey E Hinton and Ruslan R Salakhutdinov. Reducing the dimensionality of data with neural networks. *science*, 313(5786):504–507, 2006.

Menglei Hu and Songcan Chen. One-pass incomplete multi-view clustering. In *Proceedings of the AAAI conference on artificial intelligence*, volume 33, pp. 3838–3845, 2019.

Jiaqi Jin, Siwei Wang, Zhibin Dong, Xinwang Liu, and En Zhu. Deep incomplete multi-view clustering with cross-view partial sample and prototype alignment. In *Proceedings of the IEEE/CVF conference on computer vision and pattern recognition*, pp. 11600–11609, 2023.

Yann LeCun, Bernhard Boser, John S Denker, Donnie Henderson, Richard E Howard, Wayne Hubbard, and Lawrence D Jackel. Backpropagation applied to handwritten zip code recognition. *Neural computation*, 1(4):541–551, 1989.

Haobin Li, Yunfan Li, Mouxing Yang, Peng Hu, Dezhong Peng, and Xi Peng. Incomplete multi-view clustering via prototype-based imputation. *arXiv preprint arXiv:2301.11045*, 2023.

Zhenglai Li, Chang Tang, Xiao Zheng, Xinwang Liu, Wei Zhang, and En Zhu. High-order correlation preserved incomplete multi-view subspace clustering. *IEEE Transactions on Image Processing*, 31:2067–2080, 2022.

Yijie Lin, Yuanbiao Gou, Zitao Liu, Boyun Li, Jiancheng Lv, and Xi Peng. Completer: Incomplete multi-view clustering via contrastive prediction. In *Proceedings of the IEEE/CVF conference on computer vision and pattern recognition*, pp. 11174–11183, 2021.

Yijie Lin, Yuanbiao Gou, Xiaotian Liu, Jinfeng Bai, Jiancheng Lv, and Xi Peng. Dual contrastive prediction for incomplete multi-view representation learning. *IEEE Transactions on Pattern Analysis and Machine Intelligence*, 45(4):4447–4461, 2022.

Suyuan Liu, Xinwang Liu, Siwei Wang, Xin Niu, and En Zhu. Fast incomplete multi-view clustering with view-independent anchors. *IEEE Transactions on Neural Networks and Learning Systems*, 35(6):7740–7751, 2022.

Xinwang Liu, Xinzhong Zhu, Miaomiao Li, Chang Tang, En Zhu, Jianping Yin, and Wen Gao. Efficient and effective incomplete multi-view clustering. In *Proceedings of the AAAI conference on artificial intelligence*, volume 33, pp. 4392–4399, 2019.

Xinwang Liu, Miaomiao Li, Chang Tang, Jingyuan Xia, Jian Xiong, Li Liu, Marius Kloft, and En Zhu. Efficient and effective regularized incomplete multi-view clustering. *IEEE transactions on pattern analysis and machine intelligence*, 43(8):2634–2646, 2020.

Jingyu Pu, Chenhang Cui, Xinyue Chen, Yazhou Ren, Xiaorong Pu, Zhifeng Hao, Philip S Yu, and Lifang He. Adaptive feature imputation with latent graph for deep incomplete multi-view clustering. In *Proceedings of the AAAI conference on artificial intelligence*, volume 38, pp. 14633–14641, 2024.

Huayi Tang and Yong Liu. Deep safe multi-view clustering: Reducing the risk of clustering performance degradation caused by view increase. In *Proceedings of the IEEE/CVF Conference on Computer Vision and Pattern Recognition*, pp. 202–211, 2022.

Daniel J Trosten, Sigurd Lokse, Robert Jenssen, and Michael Kampffmeyer. Reconsidering representation alignment for multi-view clustering. In *Proceedings of the IEEE/CVF conference on computer vision and pattern recognition*, pp. 1255–1265, 2021.

Ashish Vaswani, Noam Shazeer, Niki Parmar, Jakob Uszkoreit, Llion Jones, Aidan N Gomez, Łukasz Kaiser, and Illia Polosukhin. Attention is all you need. *Advances in neural information processing systems*, 30, 2017.

Xinhang Wan, Bin Xiao, Xinwang Liu, Jiyuan Liu, Weixuan Liang, and En Zhu. Fast continual multi-view clustering with incomplete views. *IEEE Transactions on Image Processing*, 33:2995–3008, 2024.

Jiatai Wang, Zhiwei Xu, Xuewen Yang, Dongjin Guo, and Limin Liu. Self-supervised image clustering from multiple incomplete views via constrastive complementary generation. *IET Computer Vision*, 17(2):189–202, 2023.

Qianqian Wang, Zhengming Ding, Zhiqiang Tao, Quanxue Gao, and Yun Fu. Generative partial multi-view clustering with adaptive fusion and cycle consistency. *IEEE Transactions on Image Processing*, 30:1771–1783, 2021.

Jie Wen, Zheng Zhang, Yong Xu, Bob Zhang, Lunke Fei, and Hong Liu. Unified embedding alignment with missing views inferring for incomplete multi-view clustering. In *Proceedings of the AAAI conference on artificial intelligence*, volume 33, pp. 5393–5400, 2019.

Yuan Xie, Bingqian Lin, Yanyun Qu, Cuihua Li, Wensheng Zhang, Lizhuang Ma, Yonggang Wen, and Dacheng Tao. Joint deep multi-view learning for image clustering. *IEEE Transactions on Knowledge and Data Engineering*, 33(11):3594–3606, 2020.

Gehui Xu, Jie Wen, Chengliang Liu, Bing Hu, Yicheng Liu, Lunke Fei, and Wei Wang. Deep variational incomplete multi-view clustering: Exploring shared clustering structures. In *Proceedings of the AAAI conference on artificial intelligence*, volume 38, pp. 16147–16155, 2024.

Jie Xu, Yazhou Ren, Huayi Tang, Xiaorong Pu, Xiaofeng Zhu, Ming Zeng, and Lifang He. Multi-vae: Learning disentangled view-common and view-peculiar visual representations for multi-view clustering. In *Proceedings of the IEEE/CVF international conference on computer vision*, pp. 9234–9243, 2021.

Jie Xu, Chao Li, Yazhou Ren, Liang Peng, Yujie Mo, Xiaoshuang Shi, and Xiaofeng Zhu. Deep incomplete multi-view clustering via mining cluster complementarity. In *Proceedings of the AAAI conference on artificial intelligence*, volume 36, pp. 8761–8769, 2022a.

Jie Xu, Huayi Tang, Yazhou Ren, Liang Peng, Xiaofeng Zhu, and Lifang He. Multi-level feature learning for contrastive multi-view clustering. In *Proceedings of the IEEE/CVF conference on computer vision and pattern recognition*, pp. 16051–16060, 2022b.

Jie Xu, Chao Li, Liang Peng, Yazhou Ren, Xiaoshuang Shi, Heng Tao Shen, and Xiaofeng Zhu. Adaptive feature projection with distribution alignment for deep incomplete multi-view clustering. *IEEE Transactions on Image Processing*, 32:1354–1366, 2023.

Wenbiao Yan, Yiyang Zhou, Yifei Wang, Qinghai Zheng, and Jihua Zhu. Multi-view semantic consistency based information bottleneck for clustering. *Knowledge-Based Systems*, 288:111448, 2024a.

Xiaoqiang Yan, Zhixiang Jin, Fengshou Han, and Yangdong Ye. Differentiable information bottleneck for deterministic multi-view clustering. In *Proceedings of the IEEE/CVF conference on computer vision and pattern recognition*, pp. 27435–27444, 2024b.

Yan Yang and Hao Wang. Multi-view clustering: A survey. *Big data mining and analytics*, 1(2): 83–107, 2018.

Yi Yang and Shawn Newsam. Bag-of-visual-words and spatial extensions for land-use classification. In *Proceedings of the 18th SIGSPATIAL international conference on advances in geographic information systems*, pp. 270–279, 2010.

Jun Yin, Pei Wang, Shiliang Sun, and Zhonglong Zheng. Incomplete multi-view clustering via multi-level contrastive learning. *IEEE Transactions on Knowledge and Data Engineering*, 2025.

Honglin Yuan, Shiyun Lai, Xingfeng Li, Jian Dai, Yuan Sun, and Zhenwen Ren. Robust prototype completion for incomplete multi-view clustering. In *Proceedings of the 32nd ACM international conference on multimedia*, pp. 10402–10411, 2024.

Honglin Yuan, Yuan Sun, Fei Zhou, Jing Wen, Shihua Yuan, Xiaojian You, and Zhenwen Ren. Prototype matching learning for incomplete multi-view clustering. *IEEE Transactions on Image Processing*, 2025.

Chao Zhang, Xiuyi Jia, Zechao Li, Chunlin Chen, and Huaxiong Li. Learning cluster-wise anchors for multi-view clustering. In *Proceedings of the AAAI conference on artificial intelligence*, volume 38, pp. 16696–16704, 2024a.

Yi Zhang, Fengyu Tian, Chuan Ma, Miaomiao Li, Hengfu Yang, Zhe Liu, En Zhu, and Xinwang Liu. Regularized instance weighting multiview clustering via late fusion alignment. *IEEE Transactions on Neural Networks and Learning Systems*, 2024b.

Lihua Zhou, Guowang Du, Kevin Lue, Lizheng Wang, and Jingwei Du. A survey and an empirical evaluation of multi-view clustering approaches. *ACM Computing Surveys*, 56(7):1–38, 2024.